Geostatistical Mapping and Assessment of Iron Concentrations in Groundwater

Ebiegberi Oborie[1]* Franklin Uleh[2] Kemebaradikumo N. Ayanka[3]
1. Department of Geology, Niger Delta University, Wilberforce Island, Bayelsa State, Nigeria
2. Shekinah Soils Nigeria Limited, Port Harcourt, Rivers State
3. Ministry of Environment, Bayelsa State, Nigeria
*Email of Corresponding Author: ebixl14@gmail.com

Abstract
Iron can often be a problematic substance in water resources; its presence in water causes unpleasant odours, taste, colour, and staining on clothes. In this study, water samples (n = 70) were collected from existing boreholes within the Yenagoa area and subjected to laboratory analysis in order to examine the spatial distribution and trends of iron concentration in groundwater. Landuse/landcover (LULC) was also acquired from the Environmental Systems Research Institute (Esri) via Sentinel-2 10-Meter LULC, utilizing the geostatistical method. The distribution analysis, including the histogram and Q-Q plot, indicates a positively skewed distribution, potentially normal. A quadratic pattern in iron concentration trends was revealed using the ArcGIS 10.5 application tool. From the results, descriptive statistics present a mean of 0.35 mg/L, a standard deviation of 0.17 mg/L, and a positive skewness of 0.88. The spatial distribution map highlights areas below and above the WHO permissible concentration of 0.3 mg/L, while hotspot analysis identifies regions exceeding the standard stipulated guideline with confidence levels ranging from 90% to 99%. Comparative analysis of geostatistical models favors the Gaussian model for accurate predictions due to its low standardized mean error. The non-normally distributed iron concentration in Yenagoa suggests localized areas with elevated concentration levels. In addition, spatial analysis and LULC analysis conducted based on the laboratory results distinguished regions adhering to and those deviating from WHO guidelines, underscoring the need for targeted intervention and the importance of tailored strategies for areas with elevated accumulations. Understanding iron concentration distribution and trends is imperative for devising strategies to mitigate potential environmental and health risks.
Keywords: Geostatistics**;** Iron; Hotspot analysis, GIS; Groundwater; LULC
DOI: 10.7176/JEES/14-3-03
Publication date: April 30th 2024

1. Introduction

Access to safe and clean drinking water is crucial for human health and well-being (Oliveira, 2017; Oki and Eteh, 2018; Howard and Bartram, 2003). In Bayelsa State, Nigeria, a significant portion of the population relies on groundwater for domestic purposes (Oboshenure et al., 2019). However, concerns about groundwater quality in the Yenagoa LGA have emerged due to elevated levels of iron (Peterside et al., 2022; Nicholas, 2023; Oki and Akana 2016). High iron concentrations in drinking water can cause undesirable aesthetic issues such as discoloration, unpleasant odor, and staining. Moreover, excessive iron intake can lead to potential health complications like gastrointestinal disturbances and iron overload, a condition characterized by excessive iron accumulation in the body (World Health Organization, 2011; Siah et al., 2005). Previous studies in the region have primarily focused on assessing overall groundwater quality using basic statistical methods (Opukumo and Oki, 2021; Richard and Aseibai, 2021). While these studies provide valuable insights, they lack the spatial dimension necessary to understand the variability of iron levels across the LGA. Geostatistics offers a powerful set of tools and techniques specifically designed for analyzing and interpreting spatial data. By incorporating spatial information, geostatistical analysis can reveal patterns, trends, and potential influencing factors that might otherwise be overlooked by traditional statistical methods (Isaaks and Srivastava, 2001; Goovaerts, 1997; Banerjee et al., 2014). The Yenagoa LGA, characterized by its dense population and high dependence on groundwater for both domestic and agricultural purposes, presents a compelling case for the application of geostatistical methods. These methods can provide insights into the spatial distribution of iron levels in the groundwater, contributing to a more comprehensive understanding of the issue. By identifying spatial patterns, geostatistical analysis can facilitate the identification of areas with elevated iron concentrations, enabling targeted interventions. Understanding the spatial distribution of iron levels is crucial for implementing effective strategies to address the issue. For instance, areas with high iron concentrations can be targeted for alternative water sources or the implementation of iron removal technologies. This targeted approach is essential for protecting residents from potential health risks associated with excessive iron intake. Geostatistical methods have been widely acknowledged for their ability to unravel complex spatial patterns and guide decision-making in various fields. In the context of water quality, the work of Heuvelink (1998), Goovaerts (1999), Krige (1951), and Wackernagel (2003) underscores the importance of incorporating spatial information into the analysis. Applying geostatistical techniques in the Yenagoa LGA not only contributes to a more nuanced understanding of the spatial distribution of iron levels but also empowers policymakers and local authorities to implement targeted interventions that address specific areas of concern.

2. Materials and Methods

2.1 Study Area

The study area is Yenagoa, the capital city of Bayelsa State, Nigeria. It is located in the heart of the Niger Delta basin (Figure 1). Spanning latitudes 4˚58'30"N - 5˚3'30"N and longitudes 6˚16'0"E - 6˚22'0"E, Yenagoa boasts a population of 352,285 (National Population Commission 2006) and is projected to reach 524,400 by 2022 (https://citypopulation.de/en/nigeria/). Well-connected by roads, the city rests on low-lying terrain with a peak elevation of 37 meters (Figure 2). Farming, fishing, and small-scale sand extraction from waterways are the mainstays of the local economy (Eteh et al., 2019). Geologically, the area sits on the southwestern edge of the Niger Delta, extensively studied by Reyment (1965) and others. The basin itself formed due to a failed rift junction, marking the separation of South America and Africa and the opening of the South Atlantic (Doust & Omatsola, 1990). Rifting began in the Late Jurassic and ended in the Mid-Cretaceous (Short & Stauble, 1967). The region is riddled with faults, mostly of the thrust type.

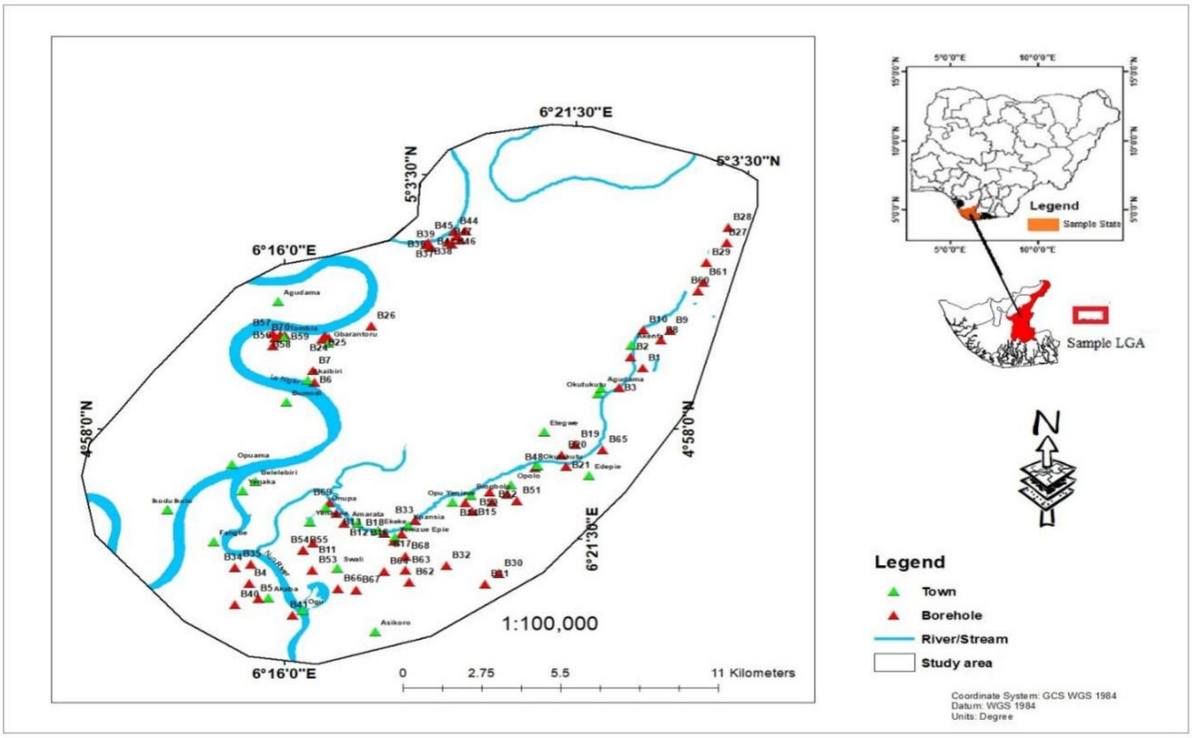

Figure 1: Sample Points within the Study Area

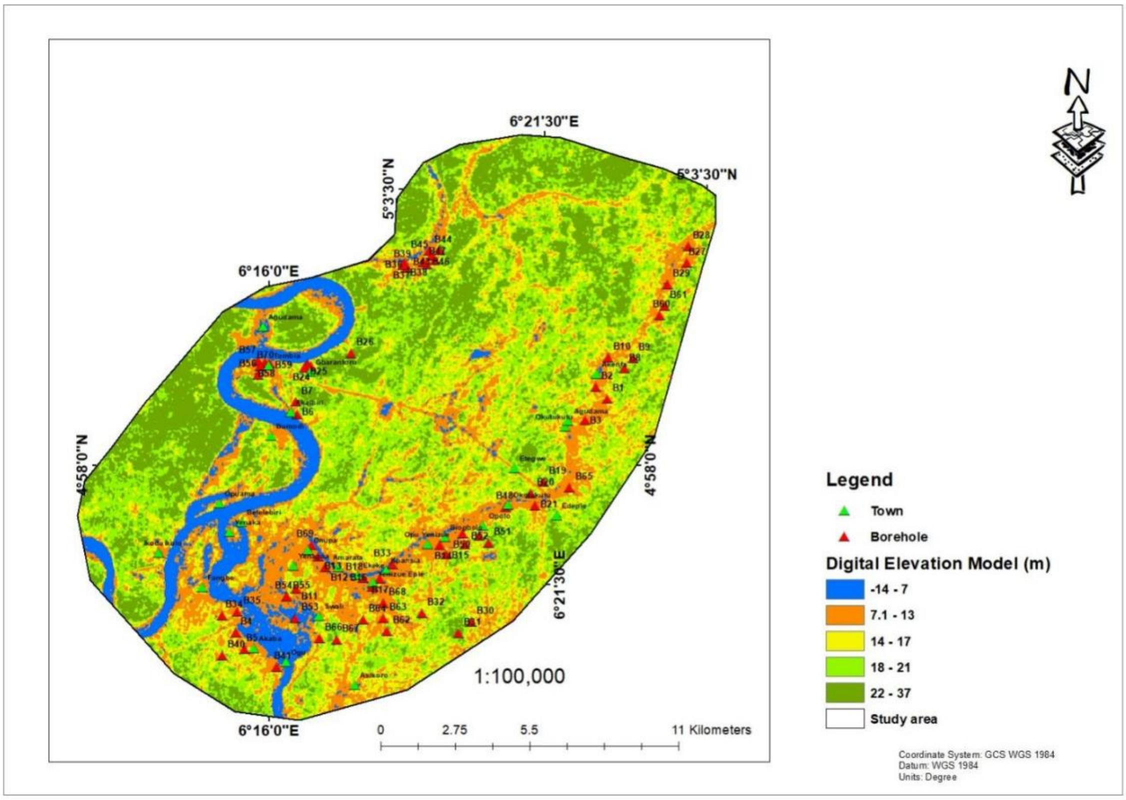

Figure 2: Digital elevation map of study area

2.2 Sample Collection and Analysis

Seventy groundwater samples were collected from boreholes strategically distributed across Yenagoa LGA, Bayelsa State, ensuring adequate coverage of the study area. The sampling locations were georeferenced using a Global Positioning System (GPS) device. Iron concentrations were determined in the laboratory using standard analytical procedures, while landuse/landcover were acquired from the Environmental Systems Research Institute (Esri) via Sentinel-2 10-Meter Land Use/Land Cover https://livingatlas.arcgis.com/landcoverexplorer/#

2.3 Geostatistical Analysis

This study employs geostatistical methods, which assume that natural phenomena can be modeled by random processes exhibiting spatial autocorrelation (Issaks and Srivastava 2001: Chowdhury et al. 2016). Through these techniques, we:

- **Predict values at unsampled locations:** This allows us to estimate the values of groundwater parameters at points where measurements were not taken.
- **Assess uncertainty in predictions:** Geostatistics provides measures of confidence in the estimated values, allowing us to understand the limitations of our predictions.
- **Model spatial patterns:** By analyzing the spatial relationships between data points, we can gain insights into the underlying processes governing the distribution of groundwater parameters.

Ordinary Kriging for interpolation: The values at unmeasured locations were calculated using Ordinary Kriging, a geostatistical interpolation method based on the concept of spatial autocorrelation (Allard ,2013). This method is used to estimate the value of a variable at an unsampled location based on its values at sampled locations.

Exploratory spatial data analysis: Before applying interpolation techniques, the data was explored using tools provided in the ArcGIS 10.5 Geostatistical Wizard. These tools include:

- **Histogram:** This provided insights into the distribution of data points, helping us understand the range and frequency of values.
- **QQPlot:** This allowed us to assess the normality of the data, which is important for certain geostatistical analyses.
- **Trend analysis:** This helped us identify any global trends or patterns in the data that might influence the spatial distribution of groundwater parameters.
- **Semivariogram:** This is a key tool in geostatistics, used to quantify the spatial autocorrelation in the data. It reveals how the similarity between data points changes as the distance between them increases.

The kriging estimate at a location x0 is given by the following formula:
$Z(x0) = \sum \lambda i * Z(xi)$
where:

- $Z(x0)$ is the estimated value at location x0
- $Z(xi)$ is the value of the variable at the i-th sampled location xi
- λi are the kriging weights assigned to each sampled point, such that they sum to 1

The weights λi are determined by minimizing the variance of the kriging estimate subject to the unbiasedness condition. This minimization problem leads to a system of linear equations that can be solved for the weights.

2.4 Model Fitting

Spatial autocorrelation, a fundamental concept in geostatistics, describes the tendency for closer things to be more alike than those farther apart. This relationship is vital for predicting unknown values in groundwater studies. Semivariograms, a statistical tool, quantify this spatial dependence. However, choosing the appropriate model for these semivariograms significantly impacts prediction accuracy. This study evaluated six models (circular, Gaussian, tetraspherical, exponential, spherical, and stable) for predicting iron (Fe) concentrations in groundwater. The best model was identified through cross-validation, considering various statistical metrics:

1. Mean Error (ME):

$$ME = \sum (y_i - \hat{y}_i) / n$$

where:

- y_i is the true value for the i-th data point
- $\hat{y}_i$ is the predicted value for the i-th data point
- n is the total number of data points

2. Root Mean Square Error (RMSE):

$$RMSE = \sqrt{\sum (y_i - \hat{y}_i)^2 / n}$$

where:

y_i and $\hat{y}_i$ are the same as in the ME formula

3. Average Standard Error (ASE):

$$ASE = \sum (SE_i) / n$$

where:

- SE_i is the standard error for the i-th data point

4. Root Mean Square Standard Error (RMSSE):

$$RMSSE = \sqrt{\sum (SE_i)^2 / n}$$

where:

- SE_i is the same as in the ASE formula

Interpretation:

- Mean error (ME): ideally close to zero for optimal model performance.
- Root mean square error (RMSE): should be close to the average standard error (ASE) for accurate predictions. High RMSE values indicate overestimation, while low values signify underestimation.
- Average standard error (ASE): This reflects the inherent variability in the data.
- Root mean square standard error (RMSSE): Values close to 1 indicate accurate predictions; values above 1 suggest overestimation, while those below 1 denote underestimation.

2.5 Spatial autocorrelation

Spatial autocorrelation analysis is conducted to explore potential factors influencing the spatial distribution of iron levels. This analysis examined the relationships between iron concentrations and various environmental variables, such as distance to rivers, elevation, and land cover types.

3. Result and Discussion

3.1 Trend Analysis

To gain deeper insights into the iron concentration in Yenagoa's groundwater, a comprehensive analysis was conducted for the year 2023. This study employed a diverse set of analytical tools to evaluate data normality and discern underlying trends, shedding light on the dynamics of iron concentration in the region.

The first step in the analysis involved a meticulous examination of the distribution of iron concentration data for the year 2023. Figure 3 is histogram that visually represents the frequency distribution of the data. Notably, both the mean and median were found to be in close proximity, suggesting a potential normal distribution. However, a closer inspection using skewness analysis uncovered a positive skew, indicating a departure from perfect normality.

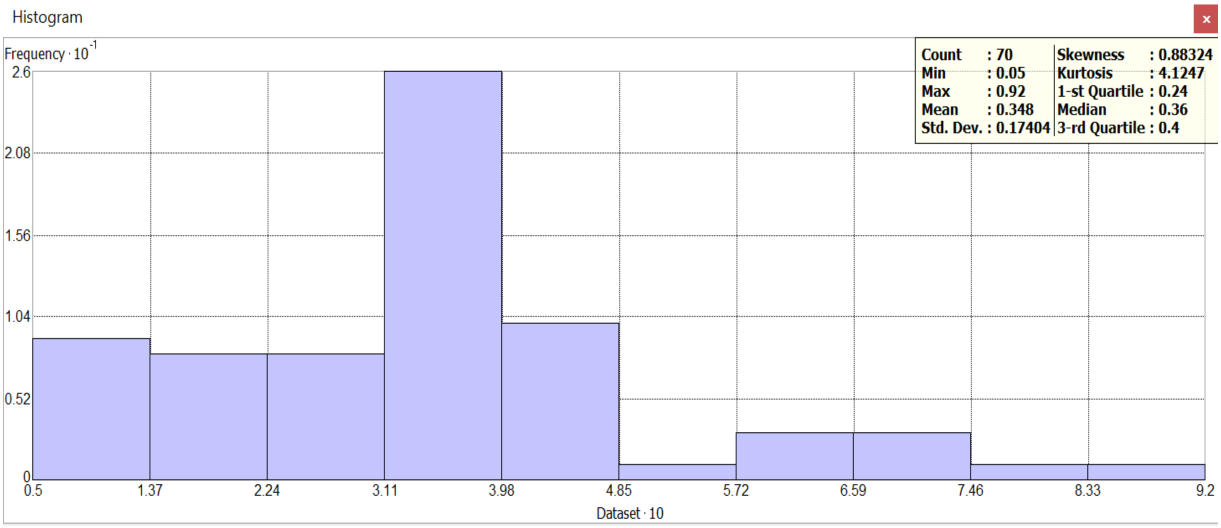

Figure 3: Histogram Plot of GroundwaterIiron Concentration Fe (mg/L)

To further validate the normal distribution, a (Q-Q) plot was generated (Figure 4a). The Q-Q plot reinforced the notion of a normal distribution, as the data points closely aligned with the expected quantiles along the straight line. This dual approach provided a nuanced understanding of the data's distribution characteristics, highlighting both the normality tendencies and the subtle skewness.

Moving beyond distribution analysis, the study delved into the identification of trends within the iron concentration data. Leveraging the ArcGIS Trend Analysis tool, a comprehensive assessment was conducted, revealing underlying patterns. When the data was rotated at 30°C, a distinctive U-shaped curve emerged, indicative of a second-degree trend. To enhance the clarity of the dataset for subsequent analysis, this trend was meticulously removed, creating a smoother surface

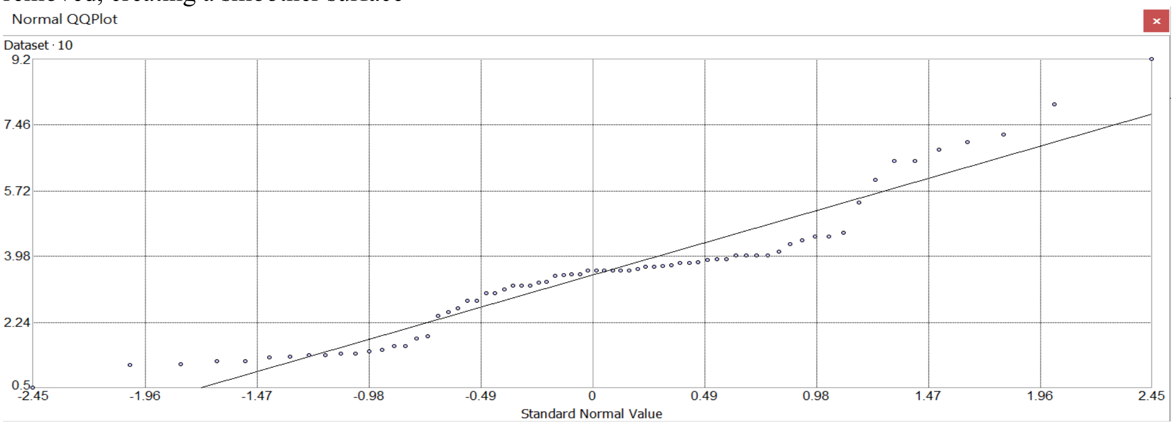

Figure 4a: Q-Q Plot Groundwater Iron Concentration Fe(mg/L).

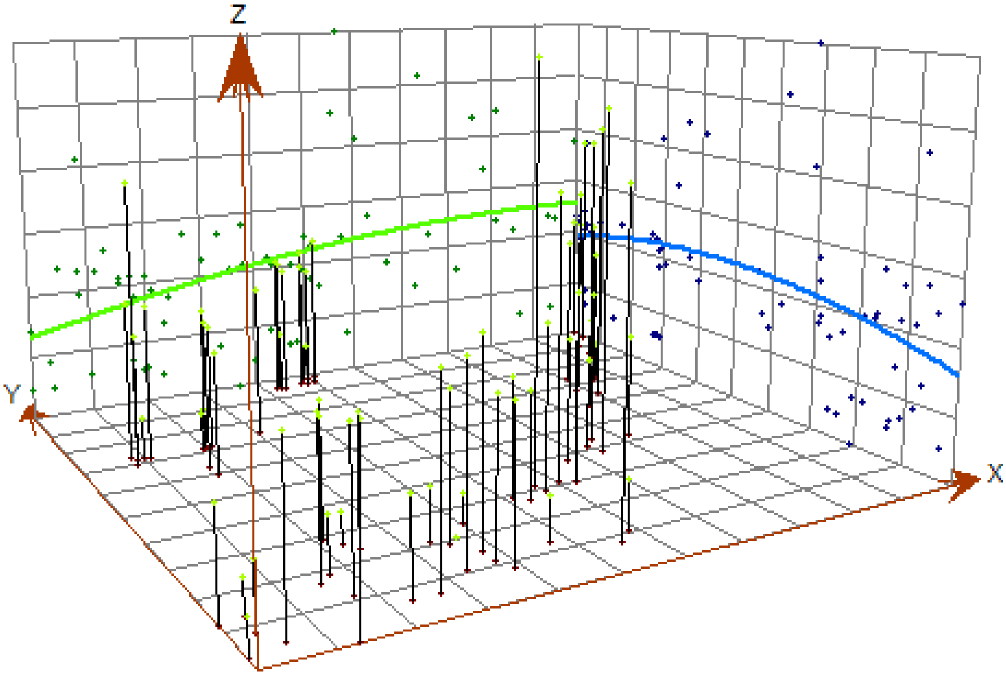

Figure 4b: Trend Analysis of Iron concentration Fe(mg/L) in Groundwater

A three-dimensional (3D) visualization technique was then employed, projecting the data onto the east-west and north-south planes (Figure 4b). The trend analysis tool was applied once again, fitting a polynomial line through the projected points. The resulting visualization showcased a conspicuous quadratic trend, depicted by the white and black lines in Figure 4. This observation unequivocally confirmed the presence of a non-linear pattern in the iron concentration data.

3.2 Iron Concentration Fe (mg/L)

Iron (Fe) is a naturally occurring element found in groundwater, but its concentration can vary significantly depending on various factors like geology, aquifer characteristics, and human activities. Understanding the spatial distribution of Fe in groundwater is crucial for assessing water quality, potential health risks, and developing effective management strategies.

This analysis focuses on Fe concentration in groundwater samples collected from a specific part of Yenagoa, Bayelsa State, Nigeria, as presented in Table 1. The Table provide descriptive statistics for Fe concentration, including the mean (0.35 mg/L), standard deviation (0.17 mg/L), and range (0.05-0.92 mg/L). Additionally, the table compares the average Fe concentration to the World Health Organization (WHO) 2011 guideline of 0.3 mg/L for drinking water.

Standard Deviation: The standard deviation of 0.174 mg/L reveals that some samples deviate significantly from the mean, potentially indicating areas with higher or lower iron concentrations.

Skewness and Kurtosis: The positive skewness value (0.88) shows that the distribution is skewed towards higher iron concentrations, with a few outliers potentially contributing to this. The kurtosis value (4.12) further indicates a distribution with heavier tails compared to a normal distribution, implying a higher probability of extreme values.

Quartiles and Median: The median iron concentration (0.36 mg/L) is slightly higher than the mean, indicate that a majority of the samples have iron levels exceeding the WHO guideline. The 1st quartile (0.24 mg/L) indicates that at least 25% of the samples have iron concentrations below the guideline.

Table 1: Descriptive statistics result of groundwater concentration of Iron in the Study area

Parameter	Value
Count	70
Minimum	0.05
Maximum	0.92
Mean	0.35
Standard Deviation	0.17
Skewness	0.88
Kurtosis	4.12
1-st Quartile	0.24
Median	0.36
World Health Organization (WHO) 2011	0.3 mg/L

3.3 Spatial distribution map

Figure 5 provides a spatial distribution map of groundwater iron concentrations, offering a visual representation of the extent of the issue. The spatial distribution map illustrates areas with concentrations ranging from 0.05 to 0.3 mg/L, denoted by a brown color. These areas fall below the World Health Organization (WHO) 2011 guideline for drinking water, set at 0.3 mg/L (Table 1). This suggests that certain regions have acceptable iron levels, providing valuable information for resource allocation and management. However, the analysis also identifies areas with iron concentrations exceeding the WHO guidelines of 67%. The color gradient in Figure 5, ranging from light brown to dark blue, signifies concentrations above the recommended limit. These areas pose a potential risk to public health, warranting immediate attention and intervention to ensure the safety of the drinking water supply.

The comparison with the hotspots map superimposed on the spatial distribution map adds complexity to the assessment. Hot spots, defined as areas with concentrations significantly higher than the surrounding regions, are identified based on statistical confidence levels. The analysis indicates that concentrations greater than 0.3 mg/L correspond to hotspots, with confidence levels ranging from 90% to 99%. Cold spots, on the other hand, represent areas where iron concentrations are significantly lower than the surrounding regions. These areas may provide insights into potential factors contributing to lower iron levels, such as geological features or effective water treatment measures. Understanding both hotspots and cold spots is crucial for developing targeted strategies to address elevated iron concentrations and ensuring equitable access to safe drinking water.

Table 2 and Figure 6 presents a comprehensive comparative analysis of six distinct geostatistical models utilized for predicting iron groundwater concentrations in a specific segment of Yenagoa, Bayelsa State. Delving into this dataset facilitates an in-depth comprehension of the merits and demerits inherent in each model within this particular context.

Examining the Mean Error of all models reveals a consistently low range from 0.0034 mg/L (Gaussian) to 0.0046 mg/L (Exponential). This implies that, on average, the predictions made by the models closely align with the actual iron concentrations in the groundwater.

The Root-Mean-Square (RMS) Error, offering insight into the variability of prediction errors, showcases similar values across all models at approximately 0.1740 mg/L. This suggests that there is no significant divergence in their capabilities to capture the distribution of actual iron concentrations.

The inclusion of Standardized Metrics, such as standardized mean and RMS errors, enables cross-model comparisons despite differing scales. The Gaussian model emerges with the lowest standardized mean error, indicating a minimized tendency to overestimate or underestimate on average. On the other hand, the exponential model boasts the lowest standardized RMS error, signifying its superior ability to effectively encapsulate the spread of errors.

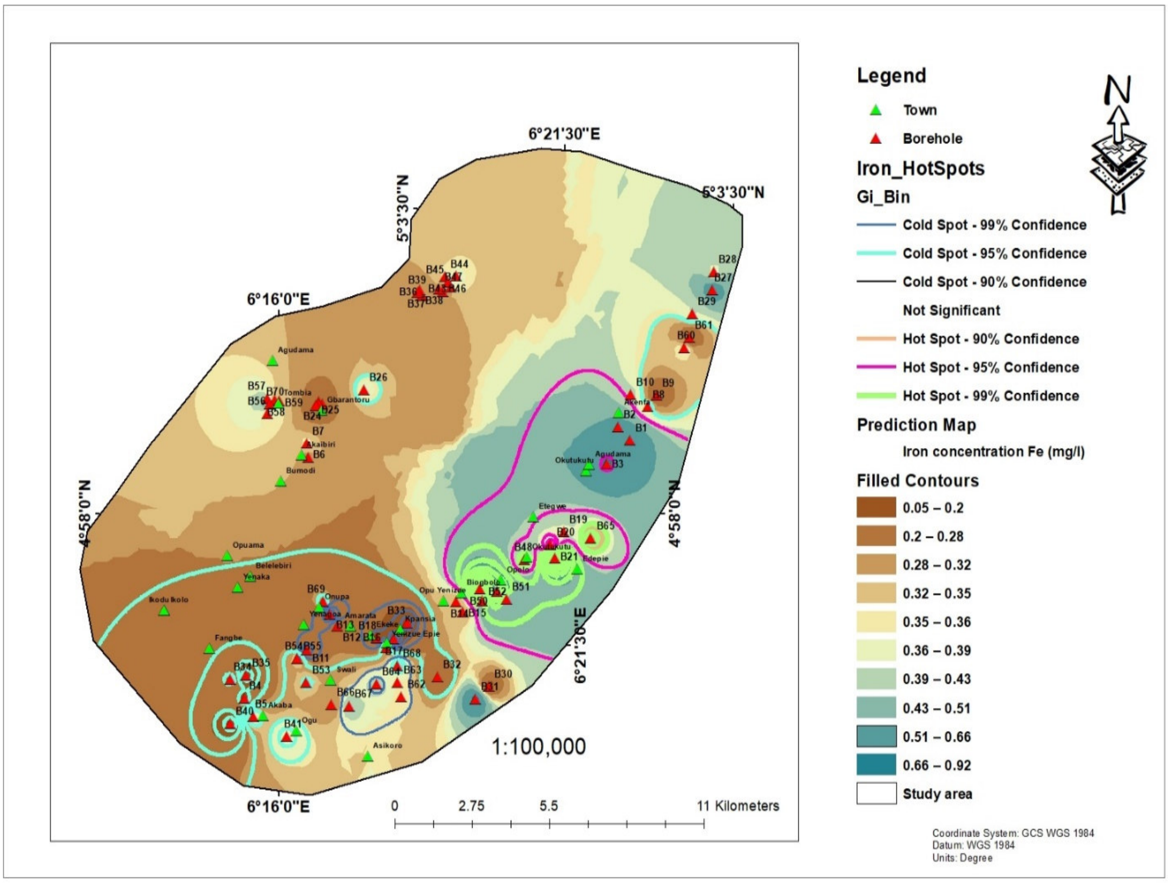

Figure 5: Hotspots and Spatial Distribution of Iron Concentration Fe(mg/L) in Groundwater

The Average Standard Error, a metric gauging the uncertainty associated with each model's predictions, reveals uniformity among all models. This suggests comparable levels of uncertainty in their forecasted values.

In evaluating Model Performance, circular and spherical models exhibit similar performance metrics, with slightly elevated mean and RMS errors compared to their counterparts. While suitable for preliminary assessments, these models may not be optimal for precise predictions. Tetraspherical and Gaussian models, however, present slightly improved performance, characterized by lower mean errors and competitive RMS errors. Among them, the Gaussian model, with its lower standardized mean error, stands out and could be considered for further in-depth analysis.

The Exponential and Stable models exhibit the lowest RMS errors, underscoring their proficiency in capturing the variability of iron concentrations. However, their higher mean and standardized mean errors suggest a predisposition to overestimate. While valuable for studies emphasizing potential contamination risks, cautious interpretation is imperative to prevent exaggeration of iron levels.

Table 2: Prediction Error for Concentration of Iron in Groundwater

Model/Error	Circular	Spherical	Tetraspherical	Exponential	Gaussian	Stable
Samples	70 of 70	70 of 70	70 of 70	70 of 70	70 of 70	70 of 70
Mean	0.0035	0.0037	0.0039	0.0046	0.0034	0.0044
Root-Mean-Square	0.1735	0.1740	0.1738	0.1740	0.1737	0.1737
Mean Standardized	0.0207	0.0215	0.0225	0.0260	0.0201	0.0248
Root-Mean-Square Standardized	1.0519	1.0550	1.0572	1.0541	1.0517	1.0527
Average Standard Error	0.1640	0.1636	0.1634	0.1636	0.1643	0.1637

3.4 Influence of land use/land cover on groundwater iron concentration

The land use/land cover in a particular area can significantly influence the groundwater iron concentration. Iron concentration in groundwater is a complex interplay of geological, hydrological, and anthropogenic factors. The land use/land cover map depicted in Figure 7 and summarized in Table 3 reveals that water constitutes 6% of the area. Iron is likely to exert minimal influence on the overall water quality in large bodies such as rivers or lakes, owing to its low solubility in well-oxygenated water. Nevertheless, smaller bodies of water, like ponds or stagnant areas, may experience higher iron concentrations, potentially affecting aquatic life. The data in Table 3, along with

Figures 7 and 8, indicate that 58% of the area is covered by vegetation. Iron, being an essential micronutrient for plant growth and vital for chlorophyll production and photosynthesis, needs to be present in adequate levels in the soil for healthy vegetation. However, excessive iron can be harmful to plants. The prevalence of vegetation suggests that iron availability likely falls within suitable ranges for most plant species. Wetlands, constituting 2% of the land use/land cover map according to Table 8 and Figure 8, typically have oxygen-depleted soils, promoting the reduction of ferric iron (Fe(III)) to ferrous iron (Fe(II)). The more soluble and mobile Fe (II) can potentially influence nutrient cycling and the plant communities adapted to wetland conditions. However, without specific data on iron concentrations and distribution, it is challenging to precisely assess the impact. Similar to vegetation, iron is crucial for crop growth. Various crop species have different iron requirements, with deficiency limiting yields and excess iron proving detrimental. Tailoring agricultural practices based on soil iron content is essential for optimal crop production. Built areas, covering 24% of the land use/land cover map as per Table 3 and Figures 7 and 8, indicate potential concentrations of iron in the environment due to construction activities and infrastructure. The impact on surrounding ecosystems depends on factors like waste management practices and potential iron leaching from construction materials. Exposed soil is susceptible to erosion, potentially leading to increased iron input into water bodies. However, the small area of bare ground suggests a minimal impact in this case. Similar to wetlands, flood vegetation often thrives in anoxic soils where Fe (II) is prevalent. Iron availability might influence specific plant communities and their ecological functions within floodplains. In rangelands, iron availability in soils can affect the composition and quality of forage for grazing animals. Deficient iron can impact animal health, while excess iron can be toxic. Understanding the iron content in rangelands is crucial for proper grazing management and animal health.

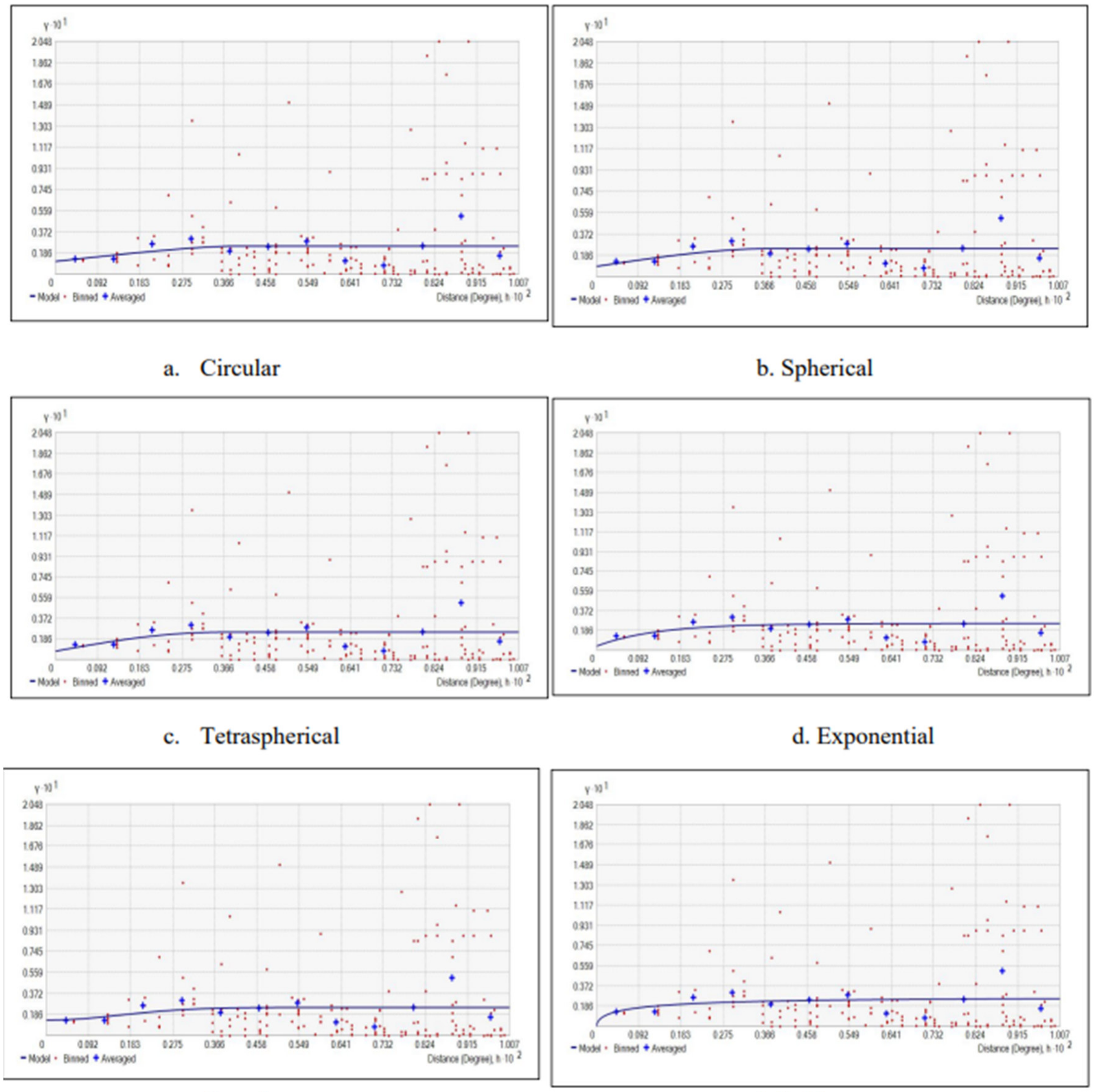

a. Circular

b. Spherical

c. Tetraspherical

d. Exponential

e. Gaussian

f. Stable

Figure 6: Fitting Model for Concentration of Iron in Groundwater

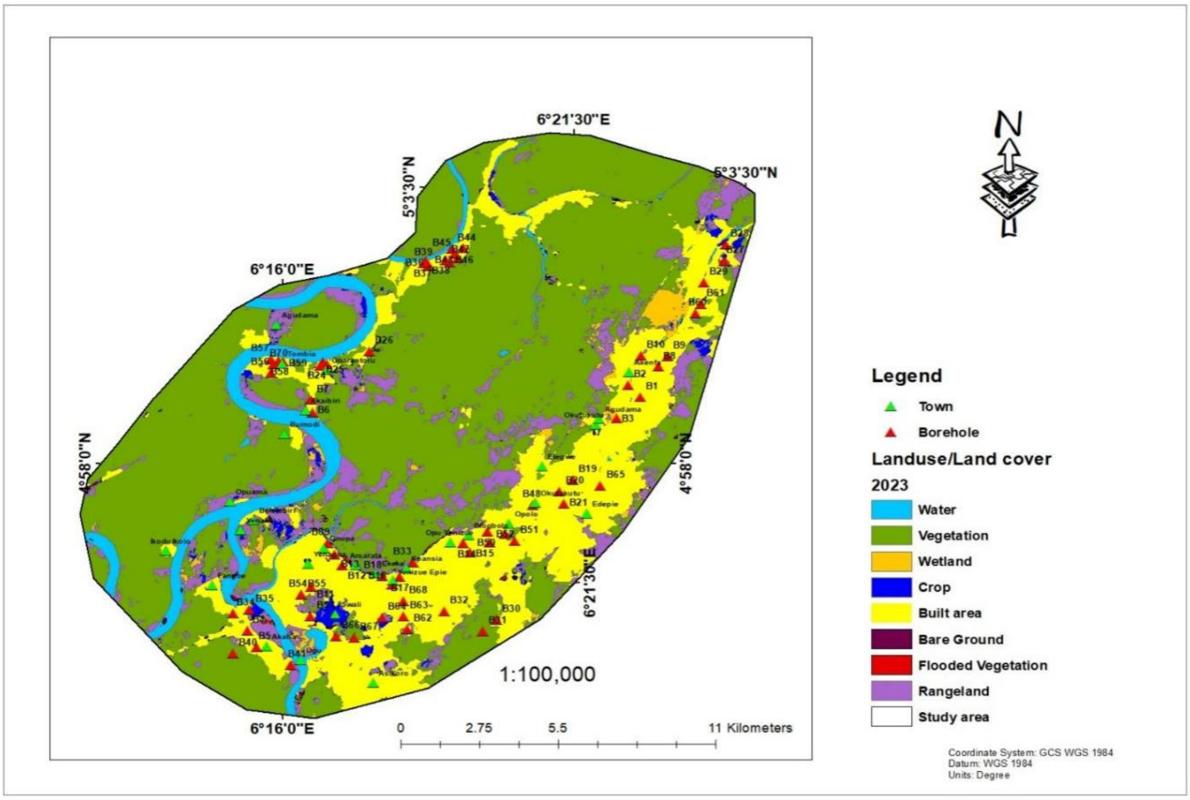

Figure 7: Landuse/land cover map in part of Yenagoa , Bayelsa State.

Table 3: land use/land cover 2023 in part of Yenagoa, Bayelsa

S/no	Classification	Area (km2)	%
1	Water	19.23	6
2	Vegetation	182.54	58
3	Wetland	5.75	2
4	Crop	4.57	1
5	Built area	76.7	24
6	Bare Ground	0.21	0
7	Flood Vegetation	0.65	0
8	Rangeland	26.83	8

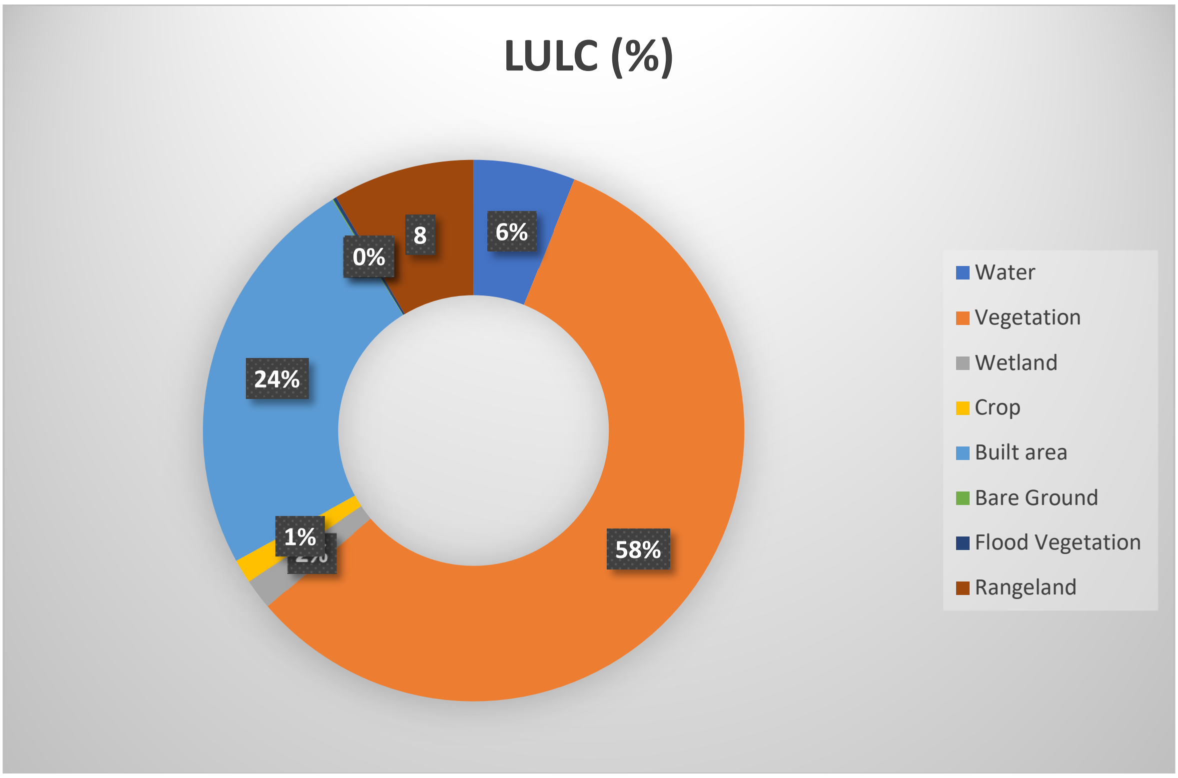

Figure 8: Percentage Chart of Landuse/land Cover map in Study Area.

3.5 Spatial Autocorrelation Analysis

Table 4 shows the results of a spatial autocorrelation analysis that examined the relationships between iron concentrations and land use/land cover in part of Yenagoa, Bayelsa. The analysis used the Global Moran's I index, which is a measure of spatial clustering.

Table 4: Spatial autocorrelation result between iron concentration and landuse /land cover

Global Moran's	Summary
Moran's Expected Index	0.129401
Expected Index	-0.00005
Variance	0.000049
Z-Score	18.43976
p-value	0

The Moran's I index is a statistic that ranges from -1 to 1. A value of -1 indicates perfect negative autocorrelation, meaning that similar values are clustered together. A value of 1 indicates perfect positive autocorrelation, meaning that dissimilar values are clustered together. A value of 0 indicates no spatial autocorrelation. The Moran's I index is positive (0.129401), which indicates that there is a positive spatial autocorrelation between iron concentrations and land use/land cover. This means that areas with high iron concentrations tend to be clustered together, and areas with low iron concentrations tend to be clustered together. The Z-score is very high (18.43976), and the p-value is very low (0.000000), which both indicate that the results are statistically significant. This means that we can be confident that the observed pattern of spatial autocorrelation is not due to chance. This finding is consistent with the idea that iron concentrations are influenced by land use/land cover. For example, industrial areas are often a source of iron pollution, so it is not surprising that areas with high iron concentrations tend to be located near industrial areas. The results of this study can be used to inform land use planning and environmental management Yenagoa, Bayelsa. For example, the finding that iron concentrations are clustered together can be used to identify areas that are at high risk of iron pollution. This information can then be used to target these areas for cleanup or to prevent future pollution.

4. Conclusion

This research aimed to gain a thorough understanding of the iron concentration distribution and trends within Yenagoa's groundwater resources. Utilizing diverse analytical tools to assess data normality, identify patterns, and forecast concentrations across different geographical areas, the study uncovered noteworthy insights. The examination of iron concentration distribution indicated a potential normal distribution, although a positive skewness value hinted at a deviation from perfect normality. The subsequent trend analysis brought attention to a quadratic trend, emphasizing non-linear patterns in the dataset. The spatial distribution map visually depicted iron concentrations across the study area, revealing regions adhering to World Health Organization (WHO) 2011 guidelines for drinking water and others surpassing recommended limits, posing potential health risks. The identification of hotspots and cold spots added complexity to the assessment, highlighting areas with significantly higher or lower concentrations. The geostatistical modeling offered a comprehensive comparison of six distinct models for predicting iron groundwater concentrations. Evaluation based on prediction errors, mean errors, and standardized metrics indicated the Gaussian model as a preferred choice for studies focusing on average iron levels and minimizing bias. However, the Exponential and Stable models, despite a tendency to overestimate, demonstrated proficiency in capturing the variability of iron concentrations with low RMS errors. The influence of land use/land cover on iron concentration was explored, revealing potential impacts on water quality, vegetation health, and animal forage. Spatial autocorrelation analysis demonstrated a positive correlation between iron concentrations and land use/land cover, offering insights for land use planning. It is imperative for authorities, policymakers, and communities to collaborate in implementing measures to mitigate the health risks associated with elevated iron levels in groundwater, ensuring a safe and sustainable water supply for all.

Reference

Allard, Denis. (2013). J.-P. Chilès, P. Delfiner: Geostatistics: Modeling Spatial Uncertainty [Book Review].

Banerjee, S., Carlin, B.P., & Gelfand, A.E. (2014). Hierarchical Modeling and Analysis for Spatial Data (2nd ed.). Chapman and Hall/CRC. https://doi.org/10.1201/b17115

Chowdhury, Tanay Datta & Zafor, Md.Abu & Chakroborty, Amit. (2016). Spatial Variation of Iron (Fe) Concentration in Groundwater of Greater Sylhet District Using Geostatistical Mapping. Nature Environment and Pollution Technology. 16.

Doust H, Omatsola E (1990). The Niger Delta. Unpublished Shell Petroleum Company Publication 1:210- 237

Environmental Systems Research Institute (Esri). (2023). Sentinel-2 10-Meter Land Use/Land Cover. Retrieved from https://livingatlas.arcgis.com/landcoverexplorer/#

Eteh D, Egobueze, Francis & Omonefe, Francis. (2019). Determination of Flood Hazard Zones Using Geographical Information Systems and Remote Sensing Techniques: A Case Study in Part Yenagoa Metropolis. Journal of Geography, Environment and Earth Science International. 1-9. 10.9734/jgeesi/2019/v21i130116.

Goovaerts, P. 1997. Geostatistics for Natural Resources Evaluation. Oxford University Press on Demand

Goovaerts, P. (1999) Geostatistics in Soil Science: State-of-the-Art and Perspectives. Geoderma, 89, 1-45. http://dx.doi.org/10.1016/S0016-7061(98)00078-0

Heuvelink, G.B.M. (1998). Error Propagation in Environmental Modelling with GIS (1st ed.). CRC Press. https://doi.org/10.4324/9780203016114

Howard, G. and Bartram, J. (2003) Domestic Water Quantity, Service, Level and Health. OMS, p. 39.

Issaks, E.H. and Srivastava, R.M. 2001. An Introduction to Applied Geostatistics. New York, USA: Oxford University Press

Krige, D.G. (1951) A Statistical Approaches to Some Basic Mine Valuation Problems on the Witwatersrand. Journal of the Chemical, Metallurgical and Mining Society of South Africa, 52, 119-139.

National Population Commission. (2006). National Population Census 2006. National Population Commission, Nigeria.

Nicholas , D. O. (2023). Spatial Analysis of Groundwater Using Geographic Information System (GIS) and Water Quality Index (WQI) in Yenagoa Local Government Area Bayelsa State, Nigeria. International Journal of Environment and Climate Change, 13(9), 1961–1977. https://doi.org/10.9734/ijecc/2023/v13i92429

Oboshenure, Kingsley & Egobueze, Francis & Egirani, Davidson. (2019). Application of GIS in the Assessment of Groundwater Quality in the Yenagoa Watershed of the Niger Delta Region of Nigeria. Asian Journal of Physical and Chemical Sciences. 1-15. 10.9734/ajopacs/2019/v7i230093.

Oki A. O. , Akana T. S. , Quality Assessment of Groundwater in Yenagoa, Niger Delta, Nigeria, Geosciences, Vol. 6 No. 1, 2016, pp. 1-12. doi: 10.5923/j.geo.20160601.01.

Oki, Austin & Rowland, Eteh. (2018). Spatial Groundwater Quality Assessment by WQI and GIS in Ogbia LGA of Bayelsa State, Nigeria. Asian Journal of Physical and Chemical Sciences. 4. 1-12. 10.9734/AJOPACS/2017/39055.

Oliveira, Celso. (2017). Sustainable access to safe drinking water: Fundamental human right in the international and national scene. Ambiente e Agua - An Interdisciplinary Journal of Applied Science. 12. 985. 10.4136/ambi-agua.2037.

Opukumo, A.W., & Oki, A.O. (2021). Assessment of Spatial Variation of Physicochemical Parameters of Groundwater in Some Communities of Yenagoa Metropolis. Journal of Geography, Environment and Earth Science International.

Peterside, A & Hart, A & Nwankwoala, Hycienth. (2022). Assessment of Groundwater Quality Using Water

Quality Index (WQI) Method in Southern Ijaw Local Government Area of Bayelsa State, Nigeria. Environmental Contaminants Reviews. 171. 35 - 48. 10.26480/ecr.02.2022.64.68.
Reyment, R.A. (1965) Aspects of the geology of Nigeria—The Stratigraphy of the Cretaceous and Cenozoic Deposits. Ibadan University Press, 133 p.
Richard, Glory & Aseibai, Ebinyo. (2021). Assessment of Mycological Quality of Groundwater in Yenagoa Metropolis, Bayelsa State, Nigeria. Sumerianz Journal of Medical and Healthcare. 76-81. 10.47752/sjmh.42.76.81.
Short, K.C. and Stauble, A.J. (1967) Outline of Geology of Niger Delta. AAPG Bulletin, 51, 761-779.
Siah, C. W., Trinder, D., & Olynyk, J. K. (2005). Iron overload. Clinica chimica acta; international journal of clinical chemistry, 358(1-2), 24–36. https://doi.org/10.1016/j.cccn.2005.02.022
Wackernagel, H. (2003) Multivariate Geostatistics: An Introduction with Applications. Springer-Verlag, Berlin. http://dx.doi.org/10.1007/978-3-662-05294-5
World Health Organization. (2011). Guidelines for drinking-water quality, 4th edition. World Health Organization